



**HAL**  
open science

# Upscaling fixed bed adsorption behaviors towards emerging micropollutants in treated natural waters with aging activated carbon Model development and validation

Ni Ye, Nicolas Cimetiere, Véronique Heim, Nils Fauchon, Cédric Feliers,  
Dominique Wolbert

## ► To cite this version:

Ni Ye, Nicolas Cimetiere, Véronique Heim, Nils Fauchon, Cédric Feliers, et al.. Upscaling fixed bed adsorption behaviors towards emerging micropollutants in treated natural waters with aging activated carbon Model development and validation. *Water Research*, 2019, 148, pp.30-40. 10.1016/j.watres.2018.10.029 . hal-01903316

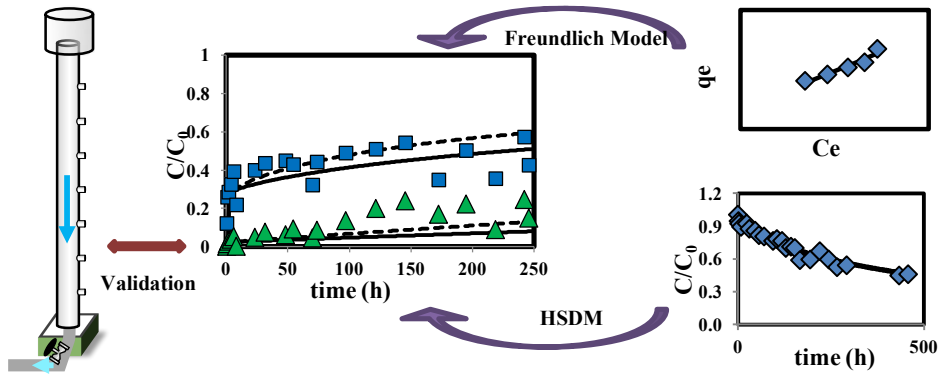
**HAL Id: hal-01903316**

**<https://univ-rennes.hal.science/hal-01903316v1>**

Submitted on 9 Nov 2018

**HAL** is a multi-disciplinary open access archive for the deposit and dissemination of scientific research documents, whether they are published or not. The documents may come from teaching and research institutions in France or abroad, or from public or private research centers.

L'archive ouverte pluridisciplinaire **HAL**, est destinée au dépôt et à la diffusion de documents scientifiques de niveau recherche, publiés ou non, émanant des établissements d'enseignement et de recherche français ou étrangers, des laboratoires publics ou privés.



1        **Upscaling fixed bed adsorption behaviors towards emerging**  
2        **micropollutants in treated natural waters with aging activated**  
3        **carbon: model development and validation**

4  
5        Ni YE<sup>\*,a,b</sup>, Nicolas CIMETIERE<sup>a</sup>, Véronique HEIM<sup>c</sup>, Nils FAUCHON<sup>b</sup>, Cédric FELIERS<sup>b</sup>,  
6        Dominique WOLBERT<sup>a</sup>

7        (a) Univ. Rennes, Ecole Nationale Supérieure de Chimie de Rennes, CNRS, ISCR - UMR  
8        6226, F - 35000 Rennes, France

9        (b) Veolia Eau d'Ile de France, 28 boulevard Pesaro, TSA 31197, 92739 Nanterre, France

10        (c) Syndicat des Eaux d'Ile de France, 120 boulevard Saint Germain, 75006 Paris

11        E-mail address: [ni.ye@veolia.com](mailto:ni.ye@veolia.com)

12                    [nicolas.cimetiere@ensc-rennes.fr](mailto:nicolas.cimetiere@ensc-rennes.fr)

13                    [v.heim@sedif.com](mailto:v.heim@sedif.com)

14                    [nils.fauchon@veolia.com](mailto:nils.fauchon@veolia.com)

15                    [cedric.feliers@veolia.com](mailto:cedric.feliers@veolia.com)

16                    [dominique.wolbert@ensc-rennes.fr](mailto:dominique.wolbert@ensc-rennes.fr)

17        \* Corresponding author:

18        E-mail address: [ni.ye@veolia.com](mailto:ni.ye@veolia.com)

19

20

## 21 **Abstract**

22 A scale-up procedure was assessed in this study to predict the fixed bed adsorption behaviors  
23 with aging granular activated carbon (GAC) for various micropollutants (pesticides,  
24 pharmaceuticals). Two assumptions of this upscaling methodology (*i.e.*, involving equal  
25 adsorption capacities and surface diffusivities between the batch test and the fixed bed) were  
26 studied for the first time to investigate the aging effect on the adsorption capacity and kinetics  
27 of carbon at full scale. This study was conducted in natural waters (the Seine River) treated by  
28 Veolia Eau d'Ile de France in Choisy-Le-Roi, a division of Syndicat des Eaux d'Ile de France,  
29 aiming to monitor real industrial conditions. The isotherms showed that the adsorption  
30 capacity for most compounds was significantly affected by aging. For the mass transfer  
31 coefficients (*i.e.*, as determined by the homogeneous surface diffusion model (HSDM)),  
32 different patterns of adsorbate/adsorbent behaviors were observed, suggesting different  
33 competition mechanisms. The model predictions (*i.e.*, HSDM) performed with all parameters  
34 obtained during the batch tests tended to overestimate the full-scale pilot adsorption  
35 performance. This overestimation could be compensated for by applying a scaling factor.  
36 Finally, an empirical pseudo-first order function was used to model the impact of the GAC  
37 service time on the characteristic adsorption parameters. Thus, our scale-up procedure may  
38 enable the prediction of long-term fixed bed adsorption behaviors and increase the model  
39 efficiency for practical implementation.

40

41 **Key words:** Adsorption; prediction; fixed bed; granular activated carbon; micropollutants;  
42 treated natural waters

43

## 44 1. Introduction

45 Adsorption on activated carbon is recognized as an efficient technology for emerging organic  
46 micropollutant (MP) removal in drinking water treatment plants (DWTPs) (Katsigiannis et al.,  
47 2015; Kennedy et al., 2015). The most common MP removal process is the application of a  
48 fixed bed reactor using granular activated carbon (GAC), where the carbon grains remain in  
49 place for several months or years. To optimize the industrial design and maintenance,  
50 numerical modeling is a useful tool to predict the MP removal efficiency. Among all the  
51 descriptive models, the homogeneous surface diffusion model (HSDM) is commonly used in  
52 number of studies to simulate adsorption processes at different scales (Bakir et al., 2014;  
53 Capelo-Neto and Buarque, 2016; Hand et al., 1997; Kim et al., 2016; Schideman et al., 2006a,  
54 2006b; Zhang et al., 2009).

55 However, the estimation of HSDM parameters (*i.e.*, adsorption capacity and kinetics) in real  
56 industrial situations is complicated by the presence of natural organic matter (NOM) in waters  
57 not only due to its direct competition but also because of its preloading effect, mainly  
58 resulting in GAC aging. Number of previous researches have assessed the NOM preloading  
59 effect, showing a reduction in the adsorption capacities and kinetics with increasing NOM  
60 preloading time (Ding et al., 2006; Li et al., 2003; Schideman et al., 2006a, 2006b).  
61 Furthermore, these studies emphasized an accurate prediction of long-term fixed bed  
62 adsorption requisites by incorporating the NOM preloading effect into the modeling process.

63 Nevertheless, these studies have some limitations. First, all of studies used artificially in-lab  
64 preloaded GAC, which may not be representative of real full-scale GAC aging, especially  
65 regarding biofilm development. Second, some of the studies were conducted with a relatively  
66 high concentration of pollutants ( $\text{mg}\cdot\text{L}^{-1}$ ), whereas the pollutant concentration in treated water  
67 (DWTP) ranges from  $\text{ng}\cdot\text{L}^{-1}$  to  $\mu\text{g}\cdot\text{L}^{-1}$ . The adsorption behavior might be different for these

68 different concentrations. To date, few modeling studies have attempted to provide insight into  
69 the effect of real fixed bed aging on pollutant adsorption at low concentrations for practical  
70 industrial implementation.

71 Various methodologies can be used to estimate the two essential HSDM parameters. Pilot-  
72 scale studies are the most accurate approach (Kennedy et al., 2015), but they are time-  
73 consuming and expensive. To overcome their disadvantages, scale-down technologies such as  
74 discontinuous tests (*i.e.*, perfectly mixed batch reactor (PMBR), differential column batch  
75 reactor (DCBR)) and short-bed column tests (SBCTs) have been investigated (Hand et al.,  
76 1984). Carter and Weber Jr. (1994) predicted the breakthrough curve of trichloroethylene in a  
77 small-scale pilot using adsorption results in batch-scale studies. Their studies demonstrated  
78 the feasibility of the upscaling method to predict fixed bed behavior; however, the studies are  
79 restricted by high pollutant concentrations, the use of artificially preloaded GAC and a  
80 relatively small-scale pilot verification.

81 Recent studies have attempted to simulate or predict full-scale pilot adsorption behavior with  
82 pollutant concentrations of  $\text{ng}\cdot\text{L}^{-1}$  or  $\mu\text{g}\cdot\text{L}^{-1}$ . Scharf et al. (2010) evaluated the adsorption  
83 capacity with ground activated carbon particles in batch tests to simulate on-site pilot test data  
84 over a two-year period. This approach is suitable for modeling but not for prediction. Later,  
85 Capelo-Neto and Buarque (2016) applied all the adsorption parameters in batch studies to  
86 predict the behavior of a hypothetical GAC filter, but the prediction results were not verified  
87 by a full-scale pilot study. Regrettably, neither study considered the NOM preloading effect in  
88 the modeling process, although the other experimental conditions approached the real DWTP  
89 conditions.

90 Hence, our study was conducted under conditions that are representative of real DWTP  
91 conditions by ensuring the same water quality as that used in real filters and ensuring a

92 pollutant concentration of  $\text{ng}\cdot\text{L}^{-1}$  to  $\mu\text{g}\cdot\text{L}^{-1}$ . In contrast to all previous studies using artificially  
93 in-lab preloaded GACs, in this study, the GAC samples were collected through local coring  
94 filters of various service times (from several months to years) at three different depths; thus,  
95 these samples represent the actual GAC spatial and temporal aging process over most of its  
96 service life.

97 The primary objective of this research is to develop and validate an upscaling methodology to  
98 predict GAC fixed bed adsorption behaviors subject to the GAC aging effect. To achieve this  
99 aim, the study is separated into three steps: (1) investigation of the GAC aging effect on the  
100 adsorption capacity and kinetics using batch tests; (2) validation of the upscaling prediction  
101 by full-scale industrial pilot tests; and (3) assessment of an empirical function of the aging  
102 effect for practical implementation.

103

## 104 **2. Materials and methods**

### 105 **2.1 Experimental methodology**

106 The choice of scale-down approaches aims to guarantee an accurate determination of  
107 adsorption parameters under controlled conditions. Adsorption isotherms were achieved using  
108 ground and mixed GAC particles in PMBR according to Capelo-Neto and Buarque (2016)  
109 and Scharf et al. (2010), with the assumption that the adsorption capacity determined by  
110 mixing GACs from three depths can approximate the overall capacity of the fixed bed. Recent  
111 works by Corwin and Summers (2010) and Kennedy et al. (2017) showed that the adsorption  
112 kinetics of MPs (*i.e.*, as for pesticides) with GAC was dominated by intraparticle diffusion  
113 (pore diffusion and surface diffusion). The external mass transfer resistance was negligible in  
114 both small-scale and pilot-scale column tests over the long term. Therefore, a differential

115 column batch reactor (DCBR) was employed here to determine the intraparticle diffusivity for  
116 uncrushed aged GAC grains. This approach can minimize the external mass transfer influence  
117 and enhance the accuracy of intraparticle diffusivity determination (Baup et al., 2000; Hand et  
118 al., 1983).

119 Finally, an *in-situ* pilot-scale test was used to validate the proposed prediction methodology.  
120 Uncrushed GACs from three depths were loaded in the same arrangement into pilot columns  
121 to approximate the real spatial variation of local filters. The columns were fed with  
122 deoxygenated water from the plant, spiked with a set of MPs.

123

## 124 **2.2 Water quality**

125 Pretreated surface water from the DWTP of Choisy-Le-Roi (France, supplying 1.8 million  
126 people for the region of Ile de France) was used for all adsorption experiments. The influent  
127 water for the pilot test was collected after the ozonation-deoxygenation step to maintain the  
128 same water quality as that in the GAC filters in the DWTP. The water used for the batch tests  
129 was collected at one time during the pilot test to minimize temporal fluctuations of influent  
130 water. In addition, 30 mg·L<sup>-1</sup> of sodium azide was added to the batch experiments to inhibit  
131 biological activities. Carter and Weber Jr. (1994) showed that the addition of sodium azide  
132 did not affect the adsorption process. Sodium azide was not added to the pilot tests to  
133 represent real industrial conditions. Previous study (Kennedy et al., 2015) also emphasized  
134 that the removal of MPs was governed by adsorption in similar conditions. Over the test  
135 period (approximately 3 weeks), the water quality was almost stable, with an average total  
136 organic carbon of approximately 2.3 mg·L<sup>-1</sup> and a pH value close to 7.9.

137



### 138 **2.3 Target MPs**

139 Seventeen emerging organic MPs, including seven pharmaceutical compounds and ten  
140 pesticides, were selected for this adsorption study in view of the MP occurrence in surface  
141 and drinking water (Gasperi et al., 2009; Vulliet et al., 2011; Vulliet and Cren-Olivé, 2011)  
142 and their removal efficiency by activated carbon (Bunmahotama et al., 2017, 2015; Mailler et  
143 al., 2016). These MPs cover a wide range of physio-chemical properties, such as molar mass,  
144 polarity and solubility to evaluate the robustness of our approach over a broad range of  
145 properties for potential targets. The detailed information is provided in Supplementary  
146 Material A (See **Table SA.1**). All compounds were of analytical purity and purchased from  
147 Sigma-Aldrich (France).

148 The selected molecules were analyzed by ultra-high-pressure liquid chromatography (UHPLC)  
149 coupled with tandem mass spectrometry (MS/MS) (Acquity, Waters, Quattro Premier,  
150 Micromass, USA) following an online solid phase extraction (SPE) (Waters 2777). The  
151 complete analytical procedure was previously described by Bazus et al. (2016) and was  
152 adapted in this study to the target compounds by a slight modification of the elution gradient.  
153 Briefly, separation was achieved within 13 minutes using an Acquity BEH C18 (2.1 x 100  
154 mm – 1.7 µm) column and with a linear elution gradient achieved by increasing the  
155 proportion of acetonitrile at a constant flow rate of 0.4 mL·min<sup>-1</sup>. The chromatographic  
156 conditions and multiple reaction monitoring (MRM) transitions are reported in **Table SA.2** in  
157 Supplementary Material A.

158

### 159 **2.4 Activated carbon**

160 To investigate the influence of GAC aging on the adsorption capacities and kinetics, a virgin  
161 GAC, namely, Aquasorb 1200 (Jacobi, France), was used as the reference for virgin GAC  
162 filters, and three aged GACs were collected from local filters at three depths (0.5 m, 1 m and  
163 2 m) from the DWTP of Choisy-Le-Roi, France. The GACs were in service for 6, 17.4 and 35  
164 months with a treated bed volume of 20930, 56000 and 102000, respectively. The four GACs  
165 were renamed C-0, C-6, C-17 and C-35, where the number represents the months of service of  
166 the GAC.

167 For the batch tests, all GAC samples were first washed with pure water to remove fines and  
168 dried at 60 °C to avoid destruction or modification of the NOM adsorbed on the GAC surface.  
169 Then, for the equilibrium isotherm test, the same amount of GAC from the three depths was  
170 mixed, crushed and sieved to obtain small-sized grains between 80 µm and 100 µm (the  
171 specific areas of the GACs are shown in **Table SA.3**) to minimize the equilibrium time and  
172 reduce the risk of degrading the target compounds. Patni et al. (2008) showed that crushed  
173 GAC had the same specific area and micropore size volume fraction as the original GAC. For  
174 batch kinetics tests, the fraction of 800/1000 µm was used by sieving the dried GAC grains of  
175 each depth separately. However, the original GAC grains were used for pilot tests without any  
176 pretreatment, and they were packed in accordance with the spatial arrangement of local filters  
177 with the same amount of GAC from the three depths.

178

## 179 **2.5 Isotherm tests and kinetics batch tests**

180 Equilibrium adsorption capacities were evaluated using the bottle-point technique. A constant  
181 mass of crushed GAC ( $2 \text{ mg}\cdot\text{L}^{-1}$ ) was mixed using magnetic stirrers with MP concentrations  
182 ranging from 1 to  $10 \text{ }\mu\text{g}\cdot\text{L}^{-1}$  in 10 L of water at room temperature (25°C). The equilibrium  
183 time was determined by following the adsorption kinetics in the middle concentration range,

184 and the kinetics evaluation showed that the adsorption reached equilibrium after 14 days.  
185 Initial and residual concentrations of each compound were measured by SPE-UPLC-MS/MS  
186 to determine the adsorption quantities according to **Eq. 1**:

$$187 \quad q_e = \frac{(C_0 - C_e) \cdot V_R}{m_{GAC}} \quad (\text{Eq. 1})$$

188 where  $q_e$  is the adsorbed quantity ( $\text{nmol} \cdot \text{g}^{-1}$ ),  $C_0$  and  $C_e$  are the initial and equilibrium solute  
189 concentrations in the liquid phase, respectively ( $\text{nmol} \cdot \text{L}^{-1}$ ),  $V_R$  is the reactor volume and  $m_{GAC}$   
190 is the quantity of GAC.

191 The kinetics studies were carried out in a DCBR with 100 mg of uncrushed GAC grains  
192 (approximately 33.3 mg for each depth). The 10 L solution ( $1 \mu\text{g} \cdot \text{L}^{-1}$  for each pollutant),  
193 which was stored in a glass bottle equipped with a magnetic stirrer, was pumped with a  
194 constant flow (peristaltic pump;  $1.5 \text{ L} \cdot \text{h}^{-1}$ ) through a small plastic column (4.32 mm inner  
195 diameter) containing the GAC grains, and then the solution was returned to the tank (**Fig.**  
196 **SB.1** in Supplementary Material B).

197

## 198 **2.6 Full-scale pilot design and experiments**

199 The full-scale pilot was designed to be representative of the GAC filter units of the DWTP in  
200 Choisy-Le-Roi, France (**Figure 1**). This pilot allows studying the breakthrough curves in 4  
201 parallel 2 m columns simultaneously fed with the same water quality. Within the plant, the  
202 water is withdrawn from the GAC feeding line into a mixing tank equipped with a back flow  
203 preventer. Since the adsorbent at the bottom of the column requires approximately the same  
204 amount of time for saturation as the GAC filters in the DWTP (typically many years),  
205 determining the complete breakthrough curve is not reasonable. Therefore, the columns were  
206 equipped with intermediate sampling points (every 25 cm) to determine the concentration-

207 depth profile at a given time or to determine the breakthrough curve at a given bed depth. The  
208 columns consist of a 50 mm internal diameter cylinder (the height of the GAC filling is  
209 approximately 1.2 m, which corresponds to an empty bed contact time of 7.2 minutes) of  
210 polycarbonate. To avoid any entry of air bubbles into the GAC filter, the columns are topped  
211 with a tank that is overflowing with water spiked with  $1 \mu\text{g}\cdot\text{L}^{-1}$  of each MP. An HPLC pump  
212 is used to add  $1.6 \text{ mL}\cdot\text{min}^{-1}$  of a  $1 \text{ mg}\cdot\text{L}^{-1}$  stock solution into the main water flow. A flow rate  
213 of  $20 \text{ L}\cdot\text{h}^{-1}$  in each column was controlled at the outlet using a multichannel peristaltic pump.  
214 The contact time and linear velocity ( $10 \text{ m}\cdot\text{h}^{-1}$ ) corresponded to the common industrial  
215 conditions of Veolia in Paris. Moreover, to ensure both a continuous operation and a reliable  
216 comparison of the GAC performance between the pilot test and the real industrial fixed bed, a  
217 2-hour backwash was applied for every 48-hour operation. Water samples were periodically  
218 collected from each column at different bed depths through sampling ports and analyzed by  
219 SPE-UPLC-MSMS.

220

## 221 **2.7 Model description**

222 Several modeling strategies have been proposed for the adsorption equilibrium of MPs in  
223 water containing NOM. Studies (Bunmahotama et al., 2017; Smith et al., 1987; Zietzschmann  
224 et al., 2014) have successfully shown the use of competition models that consider the NOM as  
225 an “equivalent background compound”. In the competition models, the optimized parameters  
226 are obtained by fitting the model parameters to experimental data associated with a defined  
227 error function. However, the application of the models is limited by common shortcomings.  
228 These models require at least mixed isotherms in NOM-free and NOM-containing water to  
229 obtain better fitting parameters. Furthermore, the fitting parameters are not transferable; hence,

230 for other water/GAC/MP system, complementary tests and fitting procedures are necessary to  
231 re-determine these parameters.

232 Another model is a single ‘apparent’ component model, which has already been employed in  
233 previous studies (Carter and Weber Jr., 1994; Scharf et al., 2010). In such a model, the  
234 parameters are directly fitted to experimental data of the target compounds obtained in NOM-  
235 containing water. Regarding the practical objective of our study, we limited ourselves to the  
236 latter approach. The adsorption equilibrium of each target molecule was modeled by the  
237 Freundlich model according to **Eq. 2**:

$$238 \quad q_e = K \times C_e^{1/n} \quad (\text{Eq. 2})$$

239 where  $q_e$  is calculated according to **Eq. 1**,  $K$  is Freundlich’s coefficient ( $\text{nmol}\cdot\text{g}^{-1}/[(\text{nmol}\cdot\text{L}^{-1})^{1/n}]$ ), and  $n$  is Freundlich’s exponent (dimensionless). The logarithmic transformation allows  
240 the use of classical linear regression available in many spreadsheet software packages.  
241

242 The HSDM was used to simulate batch kinetics and pilot breakthrough curves. The model  
243 equations for DCBR and fixed bed are presented in **Table SA.4**, and these equations were  
244 numerically solved using in-house software (Baup et al., 2000) that applied the orthogonal  
245 collocation method to convert the partial differential equations into ordinary differential  
246 equations with a function of approximation provided by Villadsen and Stewart (1967). The  
247 resolution began with nondimensionalization of the equations to simplify the influence of  
248 units. External mass transfer (characterized by the coefficient  $k_f$ ) and surface diffusion  
249 (characterized by the surface diffusion coefficient  $D_s$ ) are the two potentially limiting steps for  
250 adsorption kinetics. Their values can be determined by fitting experimental data. The  
251 optimization solver’s fitting criteria are the sum of least squares of the absolute difference  
252 between the experimental and modeled concentrations at all sampling times. The Biot number  
253 (**Eq. 3**) is introduced to interpret the predominant limiting step. When the Biot number  $> 100$ ,

254 the whole kinetics process is controlled by surface diffusion; when the Biot number  $< 0.1$ , the  
255 external mass transfer is predominant, and when the Biot number is between 0.1 and 100, the  
256 adsorption kinetics is influenced by the two mechanisms. More details of the model  
257 description can be found in many publications (Schideman et al., 2006a; Zhang et al., 2009).

$$258 \quad Biot = \frac{k_f \cdot R_p \cdot C_0}{D_s \cdot \rho_p \cdot q_0} \quad (\text{Eq. 3})$$

259 Here,  $R_p$  and  $\rho_p$  are the particulate radius and apparent density, respectively, and  $q_0$  is the  
260 adsorption capacity of carbon at concentration  $C_0$ .

261

## 262 **3. Results and discussion**

### 263 **3.1 Effect of GAC aging on the adsorption capacity**

264 The effect of GAC aging on the adsorption capacity was evaluated using isothermal  
265 equilibrium tests with a virgin GAC (C-0) and three aged GACs (C-6, C-17 and C-35). The  
266 obtained Freundlich model parameters ( $K$  and  $1/n$ ) can be found in **Table SA.5**. The  
267 adsorption capacity of compounds (represented by  $q$ ) is equal to the  $K$  value when the  
268 concentration is fixed to  $1 \text{ nmol} \cdot \text{L}^{-1}$ . To facilitate the comparison of the aging effect for  
269 different compounds, the relative adsorption capacity was introduced. Instead of using the  
270 virgin GAC as a reference, we used  $q/q_{\max}$  since some compounds have a higher  $q$  value with  
271 aged GAC than with virgin GAC.

272 **Figure 2** shows that the GAC aging effect on MP adsorption differs. Four behaviors can be  
273 distinguished. For the pollutants of Group I, a continuous decrease in  $q$  is observed with  
274 increasing aging time. The  $q$  values diminish sharply (approximate 50%) after the initial 6  
275 months of use and continue to decrease at a similar or slightly slower rate with increasing age.

276 Compounds of Group II have a similar severe reduction in  $q$  values (more than 50%) at the  
277 earlier aging stage. However, unlike Group I, the  $K$  values for these compounds remain stable  
278 afterward (between 6 and 35 months of service). The two behaviors of Groups I and II have  
279 been reported in previous studies (Carter and Weber Jr., 1994; Schideman et al., 2006a),  
280 noting that the NOM accumulated successively at the GAC surface reduced adsorption  
281 capacity due to pore blockage and pore competition.

282 For the compounds of Group III, a general reduction in  $q$  was observed for the three aged  
283 GACs compared to the virgin GAC. However, after a strong initial decrease, the  $q$  values of  
284 the three compounds increased with aging time. This irregular increase in adsorption capacity  
285 is difficult to explain with the current competition mechanisms. Changes in the nature of the  
286 biofilm might provide an explanation. Long-term studies of biofilm formation scare, but some  
287 data indicate an evolution of the morphology and composition of the biofilm (Batté et al.,  
288 2003; Gibert et al., 2013) during a long operation time, especially a reduction in the  
289 carbohydrate content from a fresh biofilm to an older biofilm. Thus, these changes in the  
290 biofilm nature might modify the affinity of GAC towards each molecule and contribute to the  
291 biodegradation of molecules.

292 In Group IV, the experimental isotherm plots (**Fig. SB.2**) show no significant difference in  
293 adsorption capacity between C-0 and C-6, whereas a serious reduction in adsorption capacity  
294 is observed after long-term use. The behavior of the compounds in this group is generally  
295 similar to the compounds of Group I but with a lag phase before the drop in the adsorption  
296 capacity. A competition mechanism mentioned by Yu et al. (2009) can explain this lag phase.  
297 At the initial preloading stage, the NOM with a low molecular weight diffuses rapidly into the  
298 adsorption sites of the outer layers of the GAC, resulting in a serious reduction in the  
299 adsorption potential of smaller molecules compared with larger molecules. As the molecules  
300 of Group IV have the highest molecular weight, they were less impacted at this initial phase

301 but could be seriously affected when the NOM diffused simultaneously into the GAC inner  
302 space during the later aging period.

303

### 304 **3.2 GAC aging influence on the adsorption kinetics**

305 The aging effect on the adsorption kinetics was first investigated by DCBR tests.

306 Experimental kinetics data obtained using the DCBR setup that was operated at initial

307 concentrations of  $1 \mu\text{g}\cdot\text{L}^{-1}$  in treated river water show no obvious difference from the aged

308 GACs (**Fig. SB.3**). However, the observed kinetics are influenced by both the adsorption

309 capacity and mass transfer. To separate these effects, the HSDM is applied using the

310 equilibrium data obtained in the previous section. The kinetics parameters are then determined

311 by fitting the external mass transfer coefficient ( $k_f$ ) and internal surface diffusivity ( $D_s$ ) to the

312 experimental data (the results are collected in **Table SA.6**).

313 The experimental plots can be satisfactorily fitted by HSDM for all pollutants, despite the

314 analytical uncertainties observed for some compounds at these low concentrations. Essentially,

315 the DCBR is designed to accurately estimate internal diffusion by minimizing or controlling

316 the influence of external diffusion. The parameter sensitivity for the model calibration is

317 interpreted by employing the Biot number. Relatively high Biot numbers ( $>50$ ) are observed

318 for most molecules (**Table SA.6**), which suggests that the adsorption kinetics is indeed

319 mainly dominated by  $D_s$ . Thus, the following discussions focus only on the influence of GAC

320 aging on  $D_s$ . A relative surface diffusivity was introduced to simplify the presentation. The

321  $D_s/D_{s\text{max}}$  ratio was also used since most compounds appear to have a higher  $D_s$  value with

322 aged GAC than with virgin GAC.



323 **Table SA.6** shows that the aging effect on  $D_s$  is complicated and might be differentiated into  
324 two groups. As presented in **Figure 3**, Group I has the highest  $D_s$  value for virgin GAC; then,  
325 this value greatly decreases at the earlier aging stage and stabilizes during the later aging  
326 period, except for diuron, whose  $D_s$  values are not greatly impacted by the aging time. The  
327 behavior of Group I was expected and has already been observed in previous studies (Carter  
328 et al., 1992; Speth and Miltner, 1989). However, the behavior of Group II was observed for  
329 the majority of molecules in which the  $D_s$  values reach the maximum after several months of  
330 use followed by a decrease in the later stage. A hypothesis is presented to explain this  
331 phenomenon. The adsorbed NOM, mainly in the macropores and mesopores, might change  
332 the surface properties, thus reducing the affinity towards some compounds. Note that the  
333 HSDM is based on the assumption that surface diffusion is largely predominant over porous  
334 diffusion (Noll et al., 1991). A less attractive surface can increase the relative contribution of  
335 porous diffusion, resulting in an apparent increase in the  $D_s$  value obtained using HSDM  
336 fitting. Indeed, the measured diffusion coefficient is an apparent coefficient that represents the  
337 two phenomena. Later in the process, the diffusion in the micropores will limit the mass  
338 transfer process. These changes in the attractiveness of the surface might differentially affect  
339 the various molecules and could explain the differences observed for the fitted  $D_s$  values.

340 The range of  $D_s$  covers several orders, making it difficult to highlight some internal  
341 correlations. The logarithmic transformation ( $pD_s = -\text{Log}_{10}(D_s)$ ) allows a better study of the  
342 possible correlations among the GACs; the results are shown in **Table SA.7**. It appears that  
343 the relationship of the  $pD_s$  values between the aged GACs and the virgin GAC is mostly  
344 insignificant (the  $p$  values are relatively high), whereas a strong linear correlation of  $pD_s$   
345 values among aged GACs is observed (**Figure 4**). Thus, for practical implementation, it  
346 seems that extrapolation of the experimental results carried out on virgin GAC to explain the

347 adsorption kinetics on aged GACs would lead to erroneous results, while the extrapolation  
348 would be much more reliable with GAC that was already exposed to NOM.

349

### 350 **3.3 Scale-up model development and validation**

351 After investigating the aging effect on the adsorption capacity and kinetics in batch tests, a  
352 scale-up procedure was carried out to predict the influence of aging on the fixed bed  
353 adsorption behavior. The procedure assumes that the GAC in the fixed bed has the same  
354 adsorption capacity and surface diffusivity as those during the batch experiment; therefore,  
355 pilot breakthrough curves can be predicted by HSDM associated with these two parameters  
356 determined in batch-scale studies. The external mass transfer coefficient is calculated by  
357 empirical correlations from the literature because it is not scalable from batch-scale studies to  
358 pilot-scale studies due to changes in flow in the reactor. The prediction results are finally  
359 verified by full-scale pilot studies.

360 Only the breakthrough curves of atenolol at the upper two depths (approximately 12 and 37  
361 cm) for 4 GACs are shown here (**Figure 5**) since the concentrations of samples taken at  
362 deeper sampling points are below the quantification limits. The results obtained for all  
363 molecules and GACs can be found in Supplemental Material B (**Fig. SB.4**). A 47% and 80%  
364 removal efficiency of atenolol was achieved for 12 cm and 37 cm depths, respectively, with  
365 virgin GAC after 250 hours of operation (**Figure 5 (a)**), corresponding to a throughput of  
366 20833 and 6757 equivalent bed volumes (BVs), respectively. However, a slightly better  
367 removal efficiency is observed for C-6 (**Figure 5 (b)**), which achieves 58% and more than 90%  
368 removal at almost the same depths. Then, the removal efficiency decreased with aging time,  
369 showing 54% and 88% for C-17 (**Figure 5 (c)**) and 41% and 72% for C-35 (**Figure 5 (d)**) at  
370 the upper two depths, respectively.

371 The observed fixed bed behaviors of atenolol with the 4 GACs are consistent with the  $D_s$   
372 evolution in the batch kinetics tests; accordingly, the better removal performance of atenolol  
373 with C-6 in the pilot tests is probably due to its faster mass transfer. The molecules penetrate  
374 more rapidly into the pores of GAC, resulting in a lower molecular concentration in the outlet  
375 flux ( $C/C_0$ ). The good agreement between the GAC adsorption behaviors in the pilot test and  
376 the  $D_s$  evolution in the batch test confirmed the feasibility of the proposed upscaling  
377 prediction procedure if the pilot-scale studies are also controlled by surface diffusion.

378 Therefore, the prediction procedure was evaluated by estimating the external mass transfer  
379 coefficient ( $k_f$ ), which was initially estimated by several empirical correlations (Ohashi et al.,  
380 1981; Ranz and Marshall Jr., 1952; Wakao and Funazkri, 1978; Wilson and Geankoplis, 1966)  
381 (**Table SA.8**) and adjusted using, in particular, the first 20 hours of the breakthrough data. It  
382 was intended to use empirical corrections for  $k_f$ ; however, the model prediction with these  
383 values underestimated the initial removal of compounds. The only adjustment of  $k_f$  improved  
384 the predictions in the early stage, which also confirmed that the film diffusion controlled the  
385 adsorption rate initially. The adjusted values (**Table SA.9**) are almost systematically 5-10  
386 times greater than their estimations by the empirical correlations, possible because the  
387 underlying assumption in the correlations is that particles are spherical, and no correction  
388 factor is incorporated into the correlation formulas to compensate for the sphericity.

389 However, **Figure 5** shows that the predicted curves with equilibrium and surface diffusion  
390 parameters obtained under batch conditions (represented by black continuous lines) are  
391 generally located below the atenolol experimental data. This finding suggests an  
392 overestimation of at least one of two “batch” parameters, either adsorption capacity or surface  
393 diffusivity, or perhaps both. Several authors (Corwin and Summers, 2010; Kennedy et al.,  
394 2017) have proposed introducing a scaling function of adsorption capacity or kinetics to  
395 compensate for this overestimation for more accurate pilot modeling.

396 Accordingly, the first step was to determine an optimized modeling procedure for the pilot  
397 results while keeping as many “batch” parameters as possible. It was decided to first adjust  
398 the  $D_s$  value and to consider modifying the equilibrium parameters only in a second stage.  
399 The reason for this choice is that the uncertainty of the surface diffusivity obtained through  
400 the batch experiments is much larger than that of the isotherm parameters since the  $D_s$  value is  
401 obtained using  $K$  and  $n$ . Another reason is that the breakthrough curves are only observed  
402 over a relatively short period (nearly two weeks), while they are mostly kinetically driven. A  
403 schematic description of the upscaling prediction procedure is shown in **Fig. SB.5**.

404 The prediction results with optimized  $D_s$  for atenolol are plotted in **Figure 5** (represented by  
405 black discontinuous lines), showing a better agreement with the experimental data. The  
406 adjusted  $D_s$  values and Biot numbers for all GACs can be found in **Table SA.9**. Similar to  
407 batch kinetics, the Biot numbers for most molecules are relatively high, indicating that surface  
408 diffusion controls the mass transfer processes for the pilot tests. This finding is in accordance  
409 with a previous study (Kennedy et al., 2017).

410 Then, the correlation analysis considers only the fitted  $k_f$  values obtained when the Biot  
411 number is below 100 because  $k_f$  values are not significant when the Biot number is greater  
412 than 100; the results are reported in **Table SA.10** and **Figure 6 (a)**. Simultaneously, a  
413 correlation analysis is also conducted with the  $pD_s$  values of the four GACs (see **Table SA.11**  
414 and **Figure 6 (b)** for the results). The results show no significant correlations of  $k_f$  or  $D_s$   
415 between the virgin GAC and the aged GACs, but good correlations are observed among the  
416 aged GACs. This result suggests that the extrapolation of  $k_f$  and  $D_s$  values for aged GACs is  
417 reliable when using GAC that was already preloaded with the NOM rather than using the  
418 virgin GAC.

419 Additionally, **Figure 7** shows that the behavior of surface diffusivity obtained by fitting fixed  
 420 bed experiments is very close to that observed from batch kinetics experiments (**Figure 3**);  
 421 their evolutions with GAC aging are similar, except for trimethoprim, ciprofloxacin and  
 422 propranolol. The cross correlations of  $pD_s$  between batch and fixed-bed tests are further  
 423 examined; however, no significant link between these tests was observed (**Figure 8**). **Figure 8**  
 424 shows that the range of variation of surface diffusion coefficients is approximately one to one  
 425 and a half orders of magnitude for the fixed bed, while it covers almost three orders of  
 426 magnitude for the batch values. Nevertheless, many points are close to the first bisector line,  
 427 indicating that for these compounds, the fixed bed  $D_s$  values can be easily obtained from the  
 428 batch data, whereas for other compounds, a scaling factor (SF) is required.

429 The investigation of the SF was then conducted for every compound and GAC, using the ratio  
 430 of the optimized pilot  $D_s$  value to the fitted DCBR  $D_s$  value. The results are summarized in  
 431 **Table SA.12**, which shows that the individual SF differs for compounds and GACs. However,  
 432 for several molecules, their individual SFs for the four GACs are very close, such as the SFs  
 433 for atenolol and atrazine, and especially for chlortoluron and diuron, whose individual SFs for  
 434 the four GACs are identical. Hence, a common SF for the four GACs was proposed by  
 435 minimizing the sum of the square error according to **Eq. 4**.

$$436 \quad \sum error = \sum \left( \frac{D_{s\ pilot} - D_{s\ DCBR} * common\ SF}{D_{s\ pilot}} \right)^2 \quad (\text{Eq. 4})$$

437 From **Table SA.12**, the 9 molecules (*i.e.*, atenolol, atrazine, chlortoluron, deisopropyl atrazine,  
 438 diuron, roxithromycin, propazine, tebuconazol) can be successfully scaled by a single  
 439 common SF ( $\sum Error < 1$ ) (an example is shown in **Figure 9**), while a common SF cannot be  
 440 derived for other molecules.

441

### 442 3.4 Application of the time-variable empirical function

443 The above studies are mainly dedicated to finding upscaling approaches for fixed bed  
 444 prediction, while the relationships among the adsorption parameters and the aging time are  
 445 not well understood. Indeed, the adsorption isotherm and kinetics tests show that the evolution  
 446 of the adsorption capacity and rate with GAC aging time can be represented by a time-  
 447 variable empirical function (Carter and Weber Jr., 1994; Jarvie et al., 2005).

448 In the study by Carter and Weber Jr. (1994), they considered up to only 4 weeks of preloading;  
 449 hence, they proposed empirical functions having a generic form like **Eq. SA.1** (in the  
 450 Supplementary Material A) or a single linear relation with preloading time. Such a model is  
 451 not suitable here, as we have observed that most kinetics parameters exhibit a maximum value  
 452 during their time evolution.

453 Moreover, several studies demonstrated that the adsorption parameters were related to the  
 454 NOM surface loading rather than the preloading time since NOM preloading can be  
 455 significantly impacted by hydraulic conditions (especially the flow velocity) (Li et al., 2003)  
 456 and the NOM concentration. Corwin and Summers (2010) showed that mixing and repacking  
 457 of GAC media did not disrupt the mass transfer zone of the NOM, and the NOM surface  
 458 concentration of a given BV was identical. Therefore, the use of a BV for the time-variable  
 459 empirical function can successfully avoid the interference of the preloading time.

460 Hence, we propose a slightly different generic expression (**Eq. 5**) that can reproduce most of  
 461 the observed evolutions; an example of the fitted curves can be seen in **Figure 10**.

$$462 \frac{X(BV)}{X_0} = 1 - (a_X - b_X \cdot BV) \cdot \exp\left(-\frac{BV}{c_X}\right) \quad (\text{Eq. 5})$$

463 where X is any adsorption parameter (K, n,  $k_f$  or  $D_s$ ) for a given BV,  $X_0$  is the value for virgin  
 464 activated carbon, and  $a_x$ ,  $b_x$  and  $c_x$  are the empirical coefficients for parameter X. Nonlinear

465 regression analyses are carried out for all varying parameters with the defined function (Eq.  
 466 5), and the results are summarized in Table SA.13 – SA.15. All coefficients here are specific  
 467 to the given adsorbate/adsorbent/matrix experimental conditions and are not to be extended to  
 468 other cases, but the empirical functions give a relatively good prediction with low errors.

469 Therefore, the GAC aging effect on the adsorption capacity and kinetics in batch tests can be  
 470 assessed by the application of a time-variable empirical function for all target molecules.  
 471 However, this assessment is not enough for a pilot prediction since the breakthrough curves of  
 472 fixed bed tests cannot be directly simulated by batch parameters without an SF. Thus, for  
 473 further upscaling applications, the empirical function of  $D_s$  can be modified by the SF (Eq. 6):

$$474 \frac{D_s(BV)_{fixed-bed}}{D_{s0,batch}} = SF \cdot \left[ 1 - (a_{D_s} - b_{D_s} \cdot BV) \cdot \exp\left(-\frac{BV}{c_{D_s}}\right) \right] \quad (\text{Eq. 6})$$

475 where the  $D_s$  value for the fixed bed prediction can be estimated at a given BV. Unfortunately,  
 476 while the values of the coefficients  $a_{D_s}$  and  $c_{D_s}$  from the DCBR data and the fixed bed data are  
 477 close for many compounds, this cannot be considered a generally acceptable assumption. A  
 478 smaller variation range of  $D_s$  values obtained from fixed bed data mainly affects the  $b_{D_s}$   
 479 values.

480

#### 481 4. Conclusions

482 The scale-up methodology based on the HSDM was tested as a feasible approach to predict  
 483 breakthrough curves of fixed beds with aged GAC. All the experiments, equilibrium, batch  
 484 kinetics and fixed bed dynamics were performed with real water that was withdrawn from a  
 485 drinking water treatment plant just before the GAC treatment unit and with the GAC sampled  
 486 from the plant's GAC filters to maximally maintain the real conditions. Several conclusions  
 487 can be drawn from this study:

- 488 • The adsorption capacities for MPs were well fitted by the Freundlich isotherm for both  
489 virgin and aged GACs in the presence of NOM. A global reduction in the adsorption  
490 capacity was observed for aged GACs compared to virgin GAC, which can be  
491 explained by pore blockage and direct competition mechanisms. While an irregular  
492 increase in the adsorption capacity was observed for three compounds with aged  
493 GACs, this result suggested that biofilm evolution modified the surface interactions  
494 towards these molecules.
- 495 • Adsorption kinetics in batch reactors and fixed bed reactors can successfully be  
496 described by HSDM for all GACs. The adsorption kinetics for both experimental  
497 scales was dominated by surface diffusion ( $D_s$ ). Instead of a continuous reduction in  
498 the  $D_s$  values with aging time, the  $D_s$  reached a maximum after several months of use  
499 for more than half of the compounds in both reactor setups. A possible explanation for  
500 this result was that modification of the surface properties by a biofilm contributed to  
501 the porous diffusion, resulting in an apparent increase in the  $D_s$  value obtained using  
502 HSDM fitting.
- 503 • The feasibility of the upscaling prediction procedure was evaluated via the adsorption  
504 capacity and surface diffusivity obtained in batch-scale tests. This modeling approach  
505 was finally verified by comparing the predicted breakthrough curves with the real  
506 adsorption profiles in a real-scale fixed bed pilot test. The model prediction  
507 overestimated the pilot adsorption performance for the majority of compounds when  
508 the batch parameters were directly used. An SF for  $D_s$  could help to compensate for  
509 the overestimation. However, its value appeared to be compound dependent. The  
510 application of the above upscaling studies for fixed bed predictions, including the  
511 direct use of batch parameters and the use of batch parameters with an SF, was



512 restricted to a portion of molecules because no clear global relationship was found  
513 between the two scales used for the experimental tests.

514 • Finally, the aging effect on the adsorption capacities and kinetics was interpreted by a  
515 new form of an empirical function that enabled reproducing the different forms of the  
516 relative evolutions of equilibrium and kinetics parameters with aging time or bed  
517 volume throughput. Although the empirical function is still an  
518 adsorbent/adsorbate/matrix-dependent function, it provides insight into the aging  
519 effect on the adsorption parameters. Combining this function with the SF, the  
520 prediction for pilot adsorption behaviors is now possible. For industrial long-term  
521 implementation, this scale-up prediction methodology associated with empirical  
522 functions should facilitate the modeling approach.

523 This simulation approach remains interesting since all modeling parameters, such as  
524 adsorption capacities and surface diffusion coefficients, determined in relatively short-term  
525 economical batch tests could be used for fixed bed efficiency predictions. Although it is  
526 beyond the scope of this study, qualitative and quantitative structure-activity relationships  
527 should be considered to interpret the influence of the nature of the compounds, the GACs or  
528 the water quality on the SF or coefficients of the time-variable empirical functions. This  
529 methodology might offer a useful simulation approach for industrial design.

530

531

## 532 **Acknowledgments**

533 We gratefully acknowledge Veolia Eau d'Ile de France (VEDIF), Syndicat des Eaux d'Ile de  
534 France (SEDIF) and the Association Nationale Recherche et Technologie (ANRT) of France

535 for the financial support. We also appreciate the cooperation of VEDIF and SEDIF for  
536 making this study possible at the drinking water treatment plant of Choisy-Le-Roi.

537

538

## 539 **Reference**

540 Bakir, A., Rowland, S.J., Thompson, R.C., 2014. Transport of persistent organic pollutants by  
541 microplastics in estuarine conditions. *Estuar. Coast. Shelf Sci.* 140, 14–21.  
542 <https://doi.org/10.1016/j.ecss.2014.01.004>

543 Batté, M., Koudjonou, B., Laurent, P., Mathieu, L., Coallier, J., Prévost, M., 2003. Biofilm  
544 responses to ageing and to a high phosphate load in a bench-scale drinking water system.  
545 *Water Res.* 37, 1351–1361. [https://doi.org/10.1016/S0043-1354\(02\)00476-1](https://doi.org/10.1016/S0043-1354(02)00476-1)

546 Baup, S., Jaffre, C., Wolbert, D., Laplanche, A., 2000. Adsorption of pesticides onto granular  
547 activated carbon: Determination of surface diffusivities using simple batch experiments.  
548 *Adsorption* 6, 219–228. <https://doi.org/10.1023/A:1008937210953>

549 Bazus, L., Cimetiere, N., Wolbert, D., Randon, G., 2016. Development of on-line solid-phase  
550 extraction-liquid chromatography coupled with tandem mass spectrometry method to  
551 quantify pharmaceutical, glucuronide conjugates and metabolites in water. *J. Chromatogr.*  
552 *Sep. Tech.* 7, 1–10. <https://doi.org/10.4172/2157-7064.1000337>

553 Bunmahotama, W., Hung, W.-N., Lin, T.-F., 2017. Prediction of the adsorption capacities for  
554 four typical organic pollutants on activated carbons in natural waters. *Water Res.* 111,  
555 28–40. <https://doi.org/10.1016/j.watres.2016.12.033>

556 Bunmahotama, W., Hung, W., Lin, T.-F., 2015. Predicting the adsorption of organic

- 557 pollutants from water onto activated carbons based on the pore size distribution and  
558 molecular connectivity index. *Water Res.* 85, 521–531.  
559 <https://doi.org/10.1016/j.watres.2015.08.008>
- 560 Capelo-Neto, J., Buarque, N.M.S., 2016. Simulation of saxitoxins adsorption in full-scale  
561 GAC filter using HSDM. *Water Res.* 88, 558–565.  
562 <https://doi.org/10.1016/j.watres.2015.10.048>
- 563 Carter, M.C., Weber Jr., W.J., 1994. Modeling adsorption of TCE by activated carbon  
564 preloaded by background organic matter. *Environ. Sci. Technol.* 28, 614–623.  
565 <https://doi.org/10.1021/es00053a013>
- 566 Carter, M.C., Weber Jr, W.J., Olmstead, K.P., 1992. Effects of background dissolved organic  
567 matter on TCE adsorption by GAC. *J. Am. Water. Assoc.* 84, 81–91.  
568 <https://doi.org/10.1002/j.1551-8833.1992.tb07415.x>
- 569 Corwin, C.J., Summers, R.S., 2010. Scaling trace organic contaminant adsorption capacity by  
570 granular activated carbon. *Environ. Sci. Technol.* 44, 5403–5408.  
571 <https://doi.org/10.1021/es9037462>
- 572 Ding, L., Mariñas, B.J., Schideman, L.C., Snoeyink, V.L., Li, Q., 2006. Competitive effects  
573 of natural organic matter: Parametrization and verification of the three-component  
574 adsorption model COMPSORB. *Environ. Sci. Technol.* 40, 350–356.  
575 <https://doi.org/10.1021/es050409u>
- 576 Gasperi, J., Garnaud, S., Rocher, V., Moilleron, R., 2009. Priority pollutants in surface waters  
577 and settleable particles within a densely urbanised area: Case study of Paris (France). *Sci.*  
578 *Total Environ.* 407, 2900–2908. <https://doi.org/10.1016/j.scitotenv.2009.01.024>
- 579 Gibert, O., Lefèvre, B., Fernández, M., Bernat, X., Paraira, M., Pons, M., 2013. Fractionation

- 580 and removal of dissolved organic carbon in a full-scale granular activated carbon filter  
581 used for drinking water production. *Water Res.* 47, 2821–2829.  
582 <https://doi.org/10.1016/j.watres.2013.02.028>
- 583 Hand, D.W., Crittenden, J.C., Hokanson, D.R., Bulloch, J.L., 1997. Predicting the  
584 performance of fixed-bed granular activated carbon adsorbers. *Water Sci. Technol.* 35,  
585 235–241. [https://doi.org/10.1016/S0273-1223\(97\)00136-4](https://doi.org/10.1016/S0273-1223(97)00136-4)
- 586 Hand, D.W., Crittenden, J.C., Thacker, W.E., 1984. Simplified models for design of fixed-bed  
587 adsorption systems. *J. Environ. Eng.* 110, 440–456.  
588 [https://doi.org/10.1061/\(ASCE\)0733-9372\(1984\)110:2\(440\)](https://doi.org/10.1061/(ASCE)0733-9372(1984)110:2(440))
- 589 Hand, D.W., Crittenden, J.C., Thacker, W.E., 1983. User-oriented batch reactor solutions to  
590 the homogeneous surface diffusion model. *J. Environ. Eng.* 109, 82–101.  
591 [https://doi.org/10.1061/\(ASCE\)0733-9372\(1983\)109:1\(82\)](https://doi.org/10.1061/(ASCE)0733-9372(1983)109:1(82))
- 592 Jarvie, M.E., Hand, D.W., Bhuvendralingam, S., Crittenden, J.C., Hokanson, D.R., 2005.  
593 Simulating the performance of fixed-bed granular activated carbon adsorbers: Removal  
594 of synthetic organic chemicals in the presence of background organic matter. *Water Res.*  
595 39, 2407–2421. <https://doi.org/10.1016/j.watres.2005.04.023>
- 596 Katsigiannis, A., Noutsopoulos, C., Mantziaras, J., Gioldasi, M., 2015. Removal of emerging  
597 pollutants through granular activated carbon. *Chem. Eng. J.* 280, 49–57.  
598 <https://doi.org/10.1016/j.cej.2015.05.109>
- 599 Kennedy, A.M., Reinert, A.M., Knappe, D.R.U., Ferrer, I., Summers, R.S., 2015. Full- and  
600 pilot-scale GAC adsorption of organic micropollutants. *Water Res.* 68, 238–248.  
601 <https://doi.org/10.1016/j.watres.2014.10.010>
- 602 Kennedy, A.M., Reinert, A.M., Knappe, D.R.U., Summers, R.S., 2017. Prediction of full-

- 603 scale GAC adsorption of organic micropollutants. *Environ. Eng. Sci.* 34, 496–507.  
604 <https://doi.org/10.1089/ees.2016.0525>
- 605 Kim, Y., Bae, J., Park, H., Suh, J.-K., You, Y.-W., Choi, H., 2016. Adsorption dynamics of  
606 methyl violet onto granulated mesoporous carbon: Facile synthesis and adsorption  
607 kinetics. *Water Res.* 101, 187–194. <https://doi.org/10.1016/j.watres.2016.04.077>
- 608 Li, Q., Mariñas, B.J., Snoeyink, V.L., Campos, C., 2003. Three-component competitive  
609 adsorption model for flow-through PAC systems. 1. Model development and verification  
610 with a PAC/membrane system. *Environ. Sci. Technol.* 37, 2997–3004.  
611 <https://doi.org/10.1021/es020989k>
- 612 Mailler, R., Gasperi, J., Coquet, Y., Derome, C., Buleté, A., Vulliet, E., Bressy, A., Varrault,  
613 G., Chebbo, G., Rocher, V., 2016. Removal of emerging micropollutants from  
614 wastewater by activated carbon adsorption: Experimental study of different activated  
615 carbons and factors influencing the adsorption of micropollutants in wastewater. *J.*  
616 *Environ. Chem. Eng.* 4, 1102–1109. <https://doi.org/10.1016/j.jece.2016.01.018>
- 617 Noll, K.E., Gounaris, V., Hou, W.-S., 1991. Adsorption technology for air and water pollution  
618 control. LEWIS PUBLISHERS, INC., Michigan, USA.
- 619 Ohashi, H., Sugawara, T., Kikuchi, K., Konno, H., 1981. Correlation of liquid-side mass  
620 transfer coefficient for single particle and fixed-beds. *J. Chem. Eng. Japan* 14, 433–438.  
621 <https://doi.org/10.1252/jcej.14.433>
- 622 Patni, A.G., Ludlow, D.K., Adams, C.D., 2008. Characteristics of ground granular activated  
623 carbon for rapid small-scale column tests. *J. Environ. Eng.* 134, 216–221.  
624 [https://doi.org/10.1061/\(ASCE\)0733-9372\(2008\)134:3\(216\)](https://doi.org/10.1061/(ASCE)0733-9372(2008)134:3(216))
- 625 Ranz, W.E., Marshall Jr., W.R., 1952. Evaporation from drops - Part 1. *Chem. Eng. Prog.* 48,

- 626 141–148. [https://doi.org/10.1016/S0924-7963\(01\)00032-X](https://doi.org/10.1016/S0924-7963(01)00032-X)
- 627 Scharf, R.G., Johnston, R.W., Semmens, M.J., Hozalski, R.M., 2010. Comparison of batch  
628 sorption tests , pilot studies , and modeling for estimating GAC bed life. *Water Res.* 44,  
629 769–780. <https://doi.org/10.1016/j.watres.2009.10.018>
- 630 Schideman, L.C., Mariñas, B.J., Snoeyink, V.L., Campos, C., 2006a. Three-component  
631 competitive adsorption model for fixed-bed and moving-bed granular activated carbon  
632 adsorbers. Part I. Model development. *Environ. Sci. Technol.* 40, 6805–6811.  
633 <https://doi.org/10.1021/es060603w>
- 634 Schideman, L.C., Mariñas, B.J., Snoeyink, V.L., Campos, C., 2006b. Three-component  
635 competitive adsorption model for fixed-bed and moving-bed granular activated carbon  
636 adsorbers. Part II. Model parameterization and verification. *Environ. Sci. Technol.* 40,  
637 6812–6817. <https://doi.org/10.1021/es060603w>
- 638 Smith, E.H., Tseng, S., Weber Jr., W.J., 1987. Modeling the adsorption of target compounds  
639 by GAC in the presence of background dissolved organic matter. *Environ. Prog.* 6, 18–  
640 25. <https://doi.org/10.1002/ep.670060119>
- 641 Speth, T.F., Miltner, R.J., 1989. Effect of preloading on the scale-up of GAC microcolumns. *J.*  
642 *Am. Water Work. Assoc.* 81, 141–148.
- 643 Villadsen, J. V., Stewart, W.E., 1967. Solution of Boundary Value Problems by Orthogonal  
644 collocation. *Chem. Eng. Sci.* 22, 1483–1501. [https://doi.org/10.1016/0009-](https://doi.org/10.1016/0009-2509(96)81831-8)  
645 [2509\(96\)81831-8](https://doi.org/10.1016/0009-2509(96)81831-8)
- 646 Vulliet, E., Cren-Olivé, C., 2011. Screening of pharmaceuticals and hormones at the regional  
647 scale, in surface and groundwaters intended to human consumption. *Environ. Pollut.* 159,  
648 2929–2934. <https://doi.org/10.1016/j.envpol.2011.04.033>

- 649 Vulliet, E., Cren-Olivé, C., Grenier-Loustalot, M.-F., 2011. Occurrence of pharmaceuticals  
650 and hormones in drinking water treated from surface waters. *Environ. Chem. Lett.* 9,  
651 103–114. <https://doi.org/10.1007/s10311-009-0253-7>
- 652 Wakao, N., Funazkri, T., 1978. Effect of fluid dispersion coefficients on particle-to-fluid mass  
653 transfer coefficients in packed beds. *Chem. Eng. Sci.* 33, 1375–1384.  
654 [https://doi.org/10.1016/0009-2509\(78\)85120-3](https://doi.org/10.1016/0009-2509(78)85120-3)
- 655 Wilson, E.J., Geankoplis, C.J., 1966. Liquid mass transfer at very low reynolds numbers in  
656 packed beds. *Ind. Eng. Chem. Fundam.* 5, 9–14. <https://doi.org/10.1021/i160017a002>
- 657 Yu, Z., Peldszus, S., Huck, P.M., 2009. Adsorption of selected pharmaceuticals and an  
658 endocrine disrupting compound by granular activated carbon. 1. Adsorption capacity and  
659 kinetics. *Environ. Sci. Technol.* 43, 1467–1473. <https://doi.org/10.1021/es801961y>
- 660 Zhang, Q., Crittenden, J., Hristovski, K., Hand, D., Westerhoff, P., 2009. User-oriented batch  
661 reactor solutions to the homogeneous surface diffusion model for different activated  
662 carbon dosages. *Water Res.* 43, 1859–1866. <https://doi.org/10.1016/j.watres.2009.01.028>
- 663 Zietzschmann, F., Worch, E., Altmann, J., Ruhl, A.S., Sperlich, A., Meinel, F., Jekel, M.,  
664 2014. Impact of EfOM size on competition in activated carbon adsorption of organic  
665 micro-pollutants from treated wastewater. *Water Res.* 65, 297–306.  
666 <https://doi.org/10.1016/j.watres.2014.07.043>

667

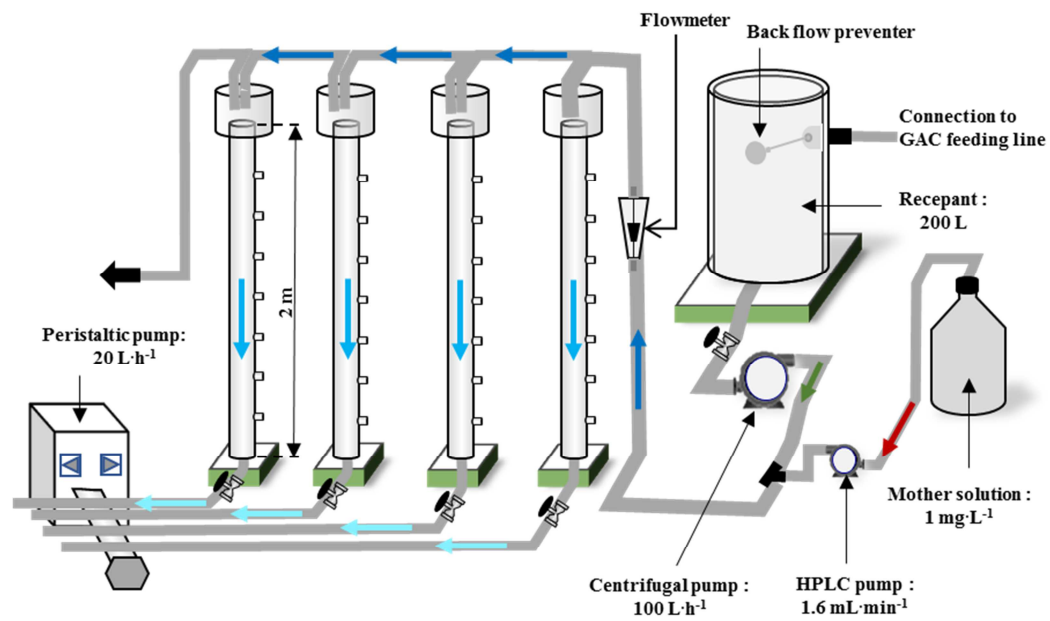


**Figure 1:** Schematic description of the full-scale pilot installation



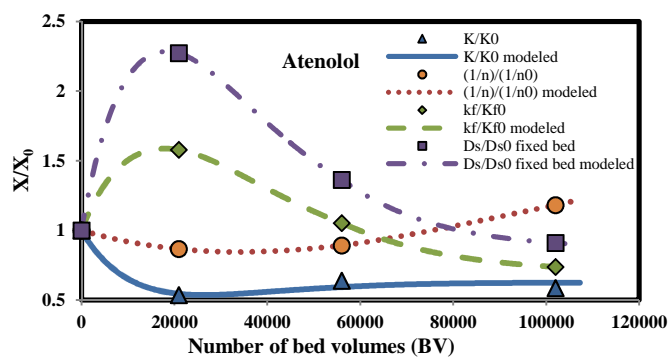


**Figure 10:** Example of fitted timely correlations for the various equilibrium and kinetic parameters of fixed bed HDSM model compared to the experimental data.

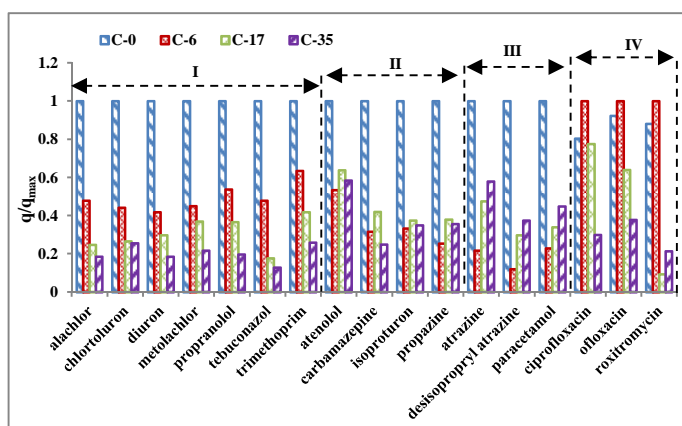


**Figure 2:** Relative adsorption capacities of micropollutants ( $q$  value compared to maximum  $q$  value of the four GACs) with various aged GACs (C-0, C-6, C-17 and C-35 represent respectively the virgin GAC and the aged GACs being in service for 6, 17 and 35 months). Four different groups of behaviors, labeled I to IV, are identified.

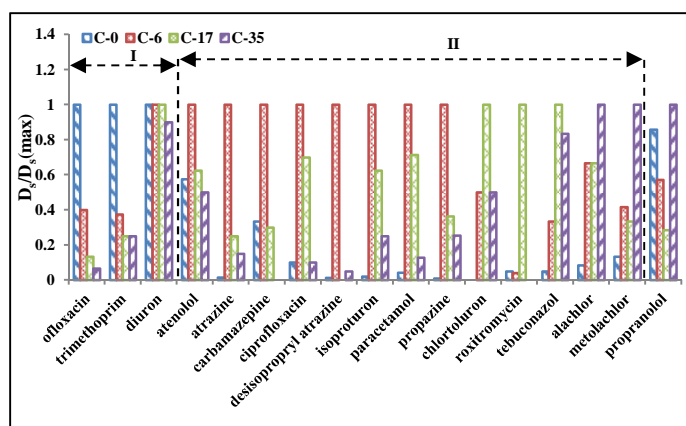


**Figure 3:** Relative surface diffusivities of micropollutants ( $D_s$  value compared to maximum  $D_s$  value of the four GACs) with various aged GACs (C-0, C-6, C-17 and C-35 represent respectively the virgin GAC and the aged GACs being in service for 6, 17 and 35 months). Two different groups of behaviors with exception of propranolol, labeled I to II, are identified.

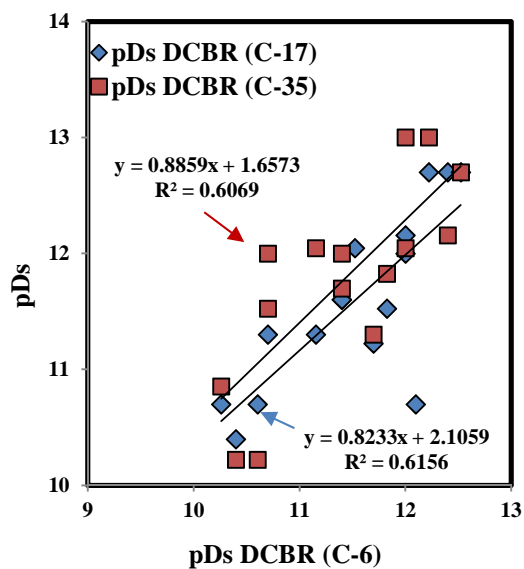


**Figure 4:** Correlation analysis of the  $pD_s$  values for DCBR setup among the aged GACs

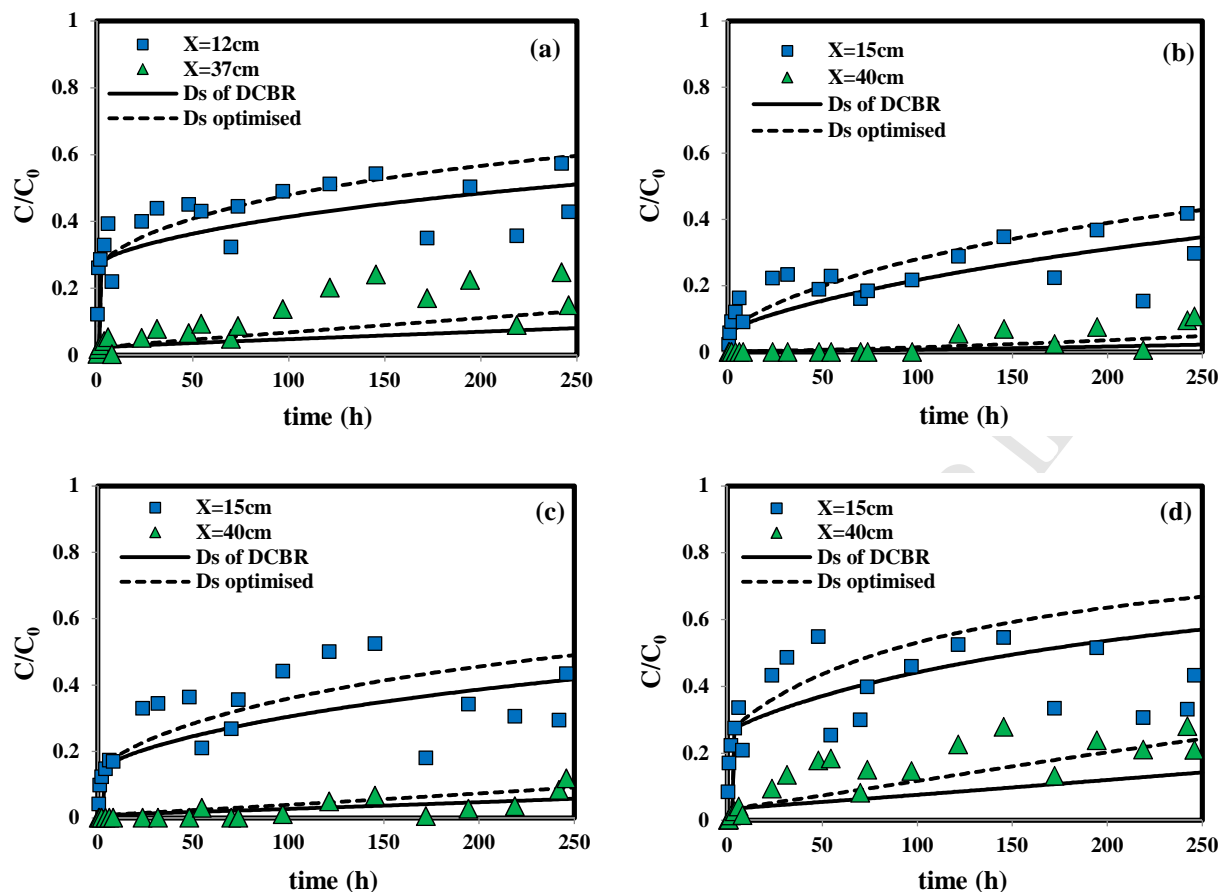


**Figure 5:** Breakthrough curves of atenolol with 4 GACs at the two depths: (a) C-0; (b) C-6; (c) C-17 and (d) C-35. Continued black line is HSDM modeling curve with  $D_s$  value obtained in DCBR setup, discontinued black line is HSDM modeling curve with optimized  $D_s$  value.

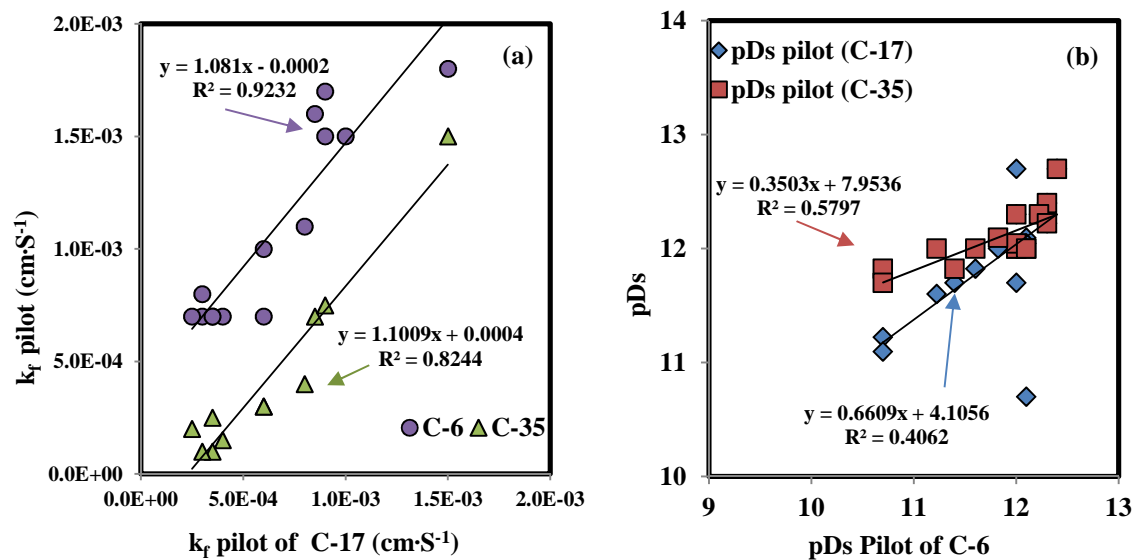


**Figure 6:** (a) Correlation among the fitted  $k_f$  values for full-scale pilot of virgin and aged GAC for the various compounds ( $k_f$  values have been discarded when the Biot number exceeded 100); (b) Correlation analysis of the  $pD_s$  values for full-scale pilot of aged GACs

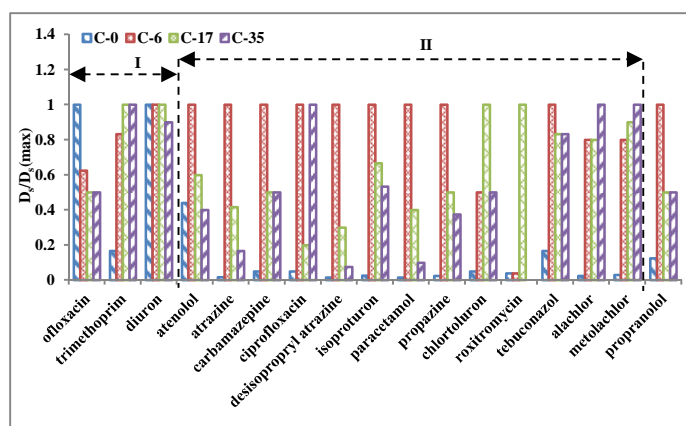


**Figure 7:** Time evolution of relative  $D_s$  values obtained from the fixed bed experiments. Group I and II are those defined in **Figure 3**.

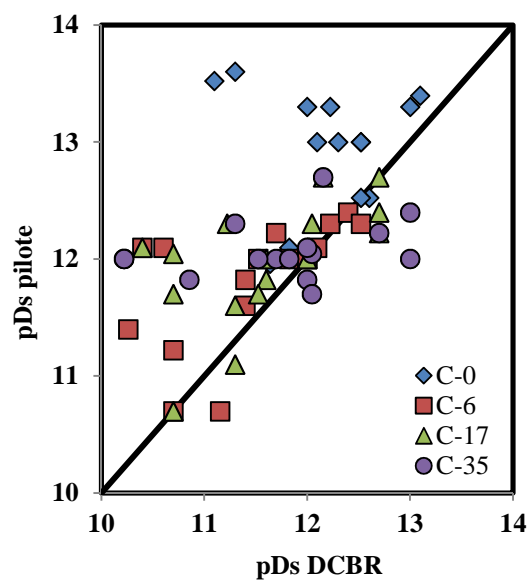


**Figure 8:** Cross correlation of  $pD_s$  values between the fixed bed and the batch kinetics tests of the 4 different GACs



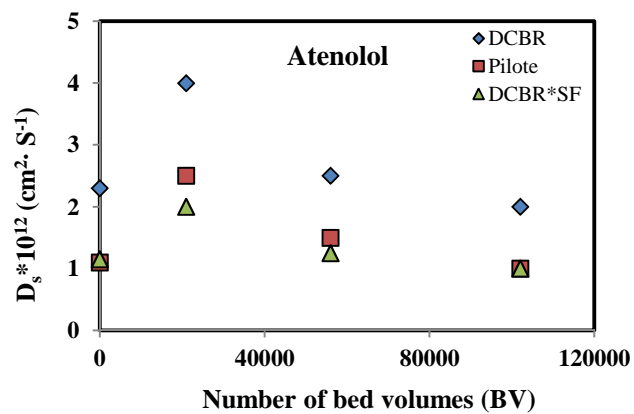


**Figure 9:** Example of application of scaling factor (SF)

**Highlights:**

- Adsorption capacities of the GAC reduced seriously after the 6 months of use
- $D_s$  reached maximum after several months of use followed by a decrease
- An SF was required to predict the adsorption behaviors of the fixed bed
- A new pseudo-first order function was employed to model the impact of GAC aging on the adsorption parameters